Loughborough University

This item was submitted to Loughborough's Research Repository by the author.
Items in Figshare are protected by copyright, with all rights reserved, unless otherwise indicated.

# Fault Tolerant Control for EMS systems with sensor failure

PLEASE CITE THE PUBLISHED VERSION

PUBLISHER

© IEEE

VERSION

VoR (Version of Record)

LICENCE

CC BY-NC-ND 4.0

REPOSITORY RECORD

Michail, Konstantinos, Argyrios C. Zolotas, Roger M. Goodall, and John T. Pearson. 2019. “Fault Tolerant Control for EMS Systems with Sensor Failure”. figshare. https://hdl.handle.net/2134/4997.

Loughborough University

This item was submitted to Loughborough's Institutional Repository (https://dspace.lboro.ac.uk/) by the author and is made available under the following Creative Commons Licence conditions.

creative commons

COMMONS DEED

**Attribution-NonCommercial-NoDerivs 2.5**

**You are free:**

- to copy, distribute, display, and perform the work

**Under the following conditions:**


**Attribution**. You must attribute the work in the manner specified by the author or licensor.

**Noncommercial**. You may not use this work for commercial purposes.

**No Derivative Works**. You may not alter, transform, or build upon this work.

- For any reuse or distribution, you must make clear to others the license terms of this work.
- Any of these conditions can be waived if you get permission from the copyright holder.

**Your fair use and other rights are in no way affected by the above.**

This is a human-readable summary of the Legal Code (the full license).

Disclaimer

For the full text of this licence, please go to:
http://creativecommons.org/licenses/by-nc-nd/2.5/

17th Mediterranean Conference on Control & Automation
Makedonia Palace, Thessaloniki, Greece
June 24 - 26, 2009

# Fault Tolerant Control for EMS systems with Sensor Failure

Konstantinos Michail
Argyrios Zolotas
and Roger Goodall
Control Systems Group,
Department of Electronic and Electrical Engineering,
Loughborough University,
Loughborough, UK, LE11 3TU
Email:k.michail@lboro.ac.uk

John Pearson
Systems Engineering Innovation Centre,
BAE Systems, Holywell Park,
Loughborough University
Loughborough, UK, LE11 3TU
Email: j.t.pearson@theiet.org

***Abstract*—The paper presents a method to recover the performance of an EMS (Electromagnetic suspension) under faulty air gap measurement. The controller is a combination of classical control loops, a Kalman estimator and analytical redundancy (for the air gap signal). In case of a faulty air gap sensor the air gap signal is recovered using the Kalman filter and analytical redundancy. Simulations verify the proposed sensor Fault Tolerant Control (FTC) method for the EMS system.**

## I. Introduction

In recent years, MAGnetic LEVitation (MAGLEV) systems have been attractive to the transport industry due to a number of advantages they offer compared to the conventional wheel-on-rail systems. In particular, maglev trains have no mechanical contacts with the rail thus reducing maintenance costs, although in general building maglev rail infrastructure is more expensive than conventional rail infrastructure [1].

MAGLEV suspensions offer high performance with desirable levels of ride quality, however they are stabilised systems and can be very sensitive to sensor faults since there is high probability of instability under sensor faults. If the EMS system becomes unstable it can either fall off or stick to the track causing possible failures of the whole system. Hence, being a critical fail-safe system substantially increases costs as it is requires a fault tolerant control structure [2].

Previous studies on fault tolerant controllers for MAGLEV suspensions, have concentrated on state feedback control [3], LMI-based $H_\infty$ approaches [4], an encounter on simultaneous stabilisation [5], as well as duplex controllers to offer some form of hardware redundancy [6]. However, this paper presents a fault tolerant control which aims to reducing hardware sensor redundancy, while optimising the overall MAGLEV performance (both deterministic and ride quality terms). In particular, the paper extends concepts presented in [7]–[9] and [10] with overall aim of simplicity in the solutions. The methodology utilises a combination of classical control with inner loop and a Kalman-busy estimator.

In order to satisfy a number of constraints simultaneously while minimising the input power to achieve the best ride quality, evolutionary algorithms have been used for the tuning of both classical controllers and Kalman filter that prove satisfactory for control applications [11]. Although the controllers and Kalman filter are designed on the linearised model of the MAGLEV vehicle, the implementation and framework validation is done on the non-linear equivalent (in order to take in account the realistic issues of varying operating conditions). The recently proposed genetic algorithm (NSGAII) based on non-dominated sorting of the individuals in the chromosome [12] has very good distribution of solutions on the optimum Pareto front and it is used in this case.

The paper is organised as follows: In section II the linearised quarter car model of the MAGLEV suspension is presented. In Section III possible disturbance inputs to the suspension followed by the MAGLEV suspension requirements and desired objectives are presented. The multiobjective constrained optimisation method using NSGAII is given in section IV while the overall problem and the approach used to implement the fault tolerant control scheme is given in Section V. Finally, the verification of the proposed method via simulations is given in Section VI followed by the conclusion in section VII.

## II. Quarter car Model

The diagram of an electromagnet suspension system is shown in Fig.1. The system represents a one degree of freedom motion and can be considered as a "quarter car" vehicle model. The suspension consists of an electromagnet with a ferromagnetic core and a coil which is attracted to the rail that is made out of ferromagnetic material. The carriage mass is attached to the electromagnet. $z_t$ is the rail position and $z$ is the carriage position. The air gap $(z_t - z)$, that is to be controlled to provide an appropriate suspension performance (see later), is the difference between the two. Assuming that the positive direction is downwards the equation of motion arising from Newton's second law is

$$M\frac{d^2z}{dt^2} = Mg - F \tag{1}$$

Where $M$ is the Mass of the carriage, $g$ is the gravity acceleration constant taken as $9.81m/s^2$ and $F$ is the vertical

978-1-4244-4685-8/09/$25.00 ©2009 IEEE


Authorized licensed use limited to: LOUGHBOROUGH UNIVERSITY. Downloaded on July 16, 2009 at 08:31 from IEEE Xplore. Restrictions apply.

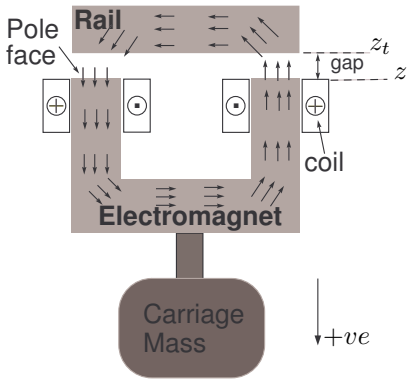


Fig. 1. Suspension system for MAGLEV

force produced by the electromagnet to keep the carriage at the operating position. The electrical circuit of the electromagnet is given by

$$u = Ri + L\frac{di}{dt} + NA\frac{db}{dt} \tag{2}$$

where, $u$ is the input voltage, $R$ is the coil's resistance, $L$ is the leakage inductance, $N$ the number of turns and $A$ is the pole face area. $i$ is the coil current and $b$ is the flux density. As indicated in [13] the four important variables in the electromagnetic suspension are Force $F$, flux density $B$, the air gap $G := G_o + (z_t - z)$ and the coil current $I$. The relationships between those variables, are shown in Fig. 2 (Straight lines for theoretical and dotted lines for a practical magnet including leakage and saturation). At constant air gap, the flux density is proportional to the coil current and at constant current is inversely proportional to the air gap. The force is proportional to the square of the flux density. The MAGLEV suspension is non-linear but there are no hard non-linearities in the system thus linear controllers can be used for control which can perform satisfactory as it is shown in section VI.

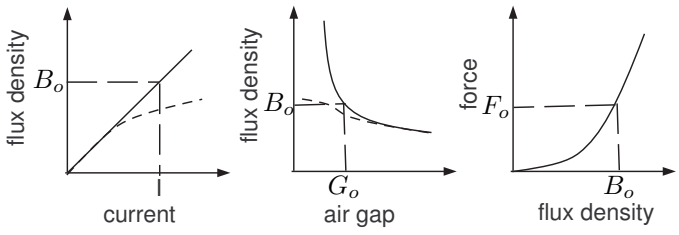


Fig. 2. MAGLEV non-linearities.

To derive the LTI state space model, linearisation is done around the operating point (nominal values) of the coil current $I_o$, flux $B_o$, force $F_o$ and nominal air gap $G_o$. The linearisation which leads to the state space model in equation (3) can be found in [7]. The state space equation is:

$$\begin{aligned} \dot{x} &= A_g x + B_u u + B_{\dot{z}_t}\dot{z}_t \\ y &= C_m x \end{aligned} \tag{3}$$

and the (linear) states are given as: $x = [i\ \dot{z}\ (z_t - z)]^T$ where $i$ is the coil current, $\dot{z}$ is the vertical velocity and $(z_t - z)$ is the air gap.
The Matrices are:

$$A_g = \begin{pmatrix} -\frac{R}{L+K_i NA} & -\frac{K_{(z_t-z)}NA}{L+K_i NA} & 0 \\ \frac{K_b K_i}{M} & 0 & -\frac{K_b K_{(z_t-z)}}{M} \\ 0 & -1 & 0 \end{pmatrix} \tag{4}$$

$$B_u = \begin{pmatrix} \frac{1}{L+K_i NA} \\ 0 \\ 0 \end{pmatrix} \quad B_{\dot{z}_t} = \begin{pmatrix} \frac{K_{(z_t-z)}NA}{L+NAK_i} \\ 0 \\ 1 \end{pmatrix} \tag{5}$$

$$C_m = \begin{pmatrix} 1 & 0 & 0 \\ K_i & 0 & -K_{(z_t-z)} \\ 0 & 0 & 1 \end{pmatrix} \tag{6}$$

where the measurements in the output matrix $(C_m)$ are the current, the flux density and the air gap $([i\ \ b\ \ (z_t - z)]^T)$. The parameter values for the quarter car model used are:$M = 1000kg$, $G_o = 0.015m$, $B_o = 1T$, $I_o = 10A$, $F_o = 9810N$, $R = 10\Omega$, $L = 0.1H$, $N = 2000$ and $A = 0.01m^2$. The constants are given as $K_i = B_o/I_o$,$K_{(z_t-z)} = B_o/G_o$ and $K_b = 2F_o/B_o$.

## III. Disturbance Inputs to the MAGLEV Suspension and Requirements

### A. Stochastic input

The stochastic input is due to random variations of the rail position as the vehicle moves along the track. These arise due to track-laying inaccuracies, steel rail discrepancies as well as due to unevenness during the installation of the rails. Considering the vertical direction, the velocity variations can be approximated by a double-sided power spectrum density (PSD) expressed as:

$$S_{\dot{z}_t} = \pi A_r V_v \tag{7}$$

where $V_v$ is the vehicle speed (taken as $15m/s$ in this case) and $A_r$ represents the roughness and is assigned a value of $1 \times 10^{-7}m$ for high quality track. The corresponding autocorrelation function is then given as:

$$R(\tau) = 2\pi^2 A_r V_v \delta(\tau) \tag{8}$$

Since a non-linear model is used for the simulations, the rms values of the variables (i.e ride quality, input current) are calculated from the values of the time history.

### B. Deterministic input

The main deterministic input to the suspension in the vertical direction is due to the transition onto a gradient. In this work, the deterministic input shown in Fig.3 is used that represents a gradient of $5\%$ at a vehicle speed of $15m/s$, an acceleration of $0.5m/s^2$ and a jerk of $1m/s^3$.



Authorized licensed use limited to: LOUGHBOROUGH UNIVERSITY. Downloaded on July 16, 2009 at 08:31 from IEEE Xplore. Restrictions apply.

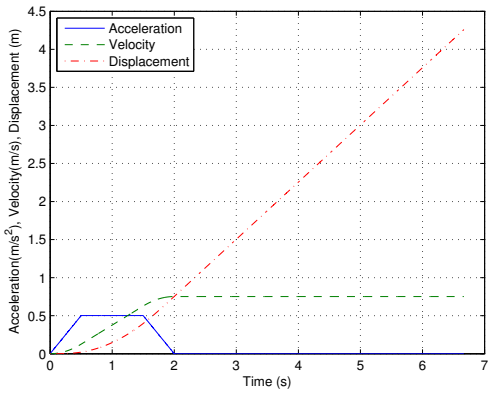


Fig. 3. Deterministic input to the suspension with a vehicle speed of $15ms^{-1}$ and 5% gradient.

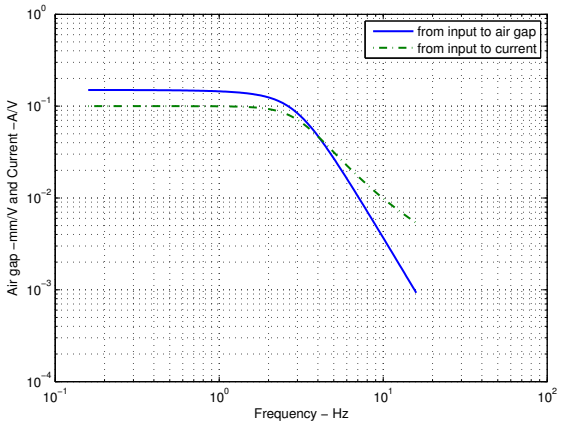


Fig. 4. Frequency response from the control input to the air gap/current outputs.

### C. Design requirements

Fundamentally there is a trade off between the deterministic (track gradient) and the stochastic response (ride quality) of the suspension. For slow speed vehicles, performance requirements are described in [14] and [15]. For this case, the objective is to minimize both the vertical acceleration, $\ddot{z}$, (improve ride quality) and the excitation of the electromagnets by minimizing RMS of the current variations $(i_{rms})$ about the nominal point. Therefore, the objective functions are given as:

$$\phi_1 = i_{rms} \quad \phi_2 = \ddot{z}_{rms} \tag{9}$$

Classical control with inner loop flux feedback is advantageous in controlling a MAGLEV vehicle [16]. Using a Proportional-Integral controller for the inner loop and Phase advance controller for the outer loop, the MAGLEV suspension can perform satisfactorily with sufficient robustness [16].

In any real application the sensors add noise to the measured quantities. For the MAGLEV suspension, the noise from sensors can be amplified by the controller and appears on the control signal (at the driving signal of the suspension). Particularly, if the controller has high gains, then the amplitude of the noise can become very large. Figure 4 shows the open-loop frequency response from the control input $(u)$ to the air gap $(mm)$ and the current $(i)$. It can be seen that the open-loop frequency response has a low pass filter characteristics and therefore the noise is filtered having limited effect at the outputs. Although the MAGLEV suspension can be considered as a low pass filter, it is better to keep the level of the noise as low as possible with an extra objective added to the optimisation algorithm:

$$\phi_3 = u_{noise_{rms}} \tag{10}$$

The required limitations are listed on table I.

TABLE I
CONSTRAINTS REQUIRED FOR THE SUSPENSION SYSTEM.

| Constrains | Value |
|---|---|
| RMS acceleration($\simeq 5\%'g'$),$(\ddot{z}_{rms})$ | $< 0.5ms^{-2}$ |
| RMS air-gap variation, $((z_t - z)_{rms})$ | $< 5mm$ |
| Max air-gap deviation (det),$(z_t - z)_p$ | $< 7.5mm$ |
| Control effort (det),$(u_p)$ | $< 300V(3I_0R_0)$ |
| Settling time, $(t_s)$ | $< 3s$ |
| Phase margin, (PM) | $35^o < PM < 45^o$ |
| Outer bandwidth $(f_{b_{in}})$ | $f_{b_{in}}\{^{<100Hz}_{>50Hz}$ |
| Inner bandwidth $(f_{b_{out}})$ | $< 10Hz$ |

## IV. MULTIOBJECTIVE CONSTRAINED OPTIMISATION VIA NSGAII

The **N**on-dominated **S**orting **G**enetic **A**lgorithm II (NSGAII) [12] is used in this paper. A summary of the basic parameter values for this algorithm are given below, while more details about the algorithm functionality can be found in [8].

The crossover probability is generally selected to be large in order to have a good mixing of genetic material. The mutation probability is defined as $1/n_v$, where $n_v$ is the number of variables. For the simulated binary crossover parameter (SBX) and the mutations parameter it was decided to use the default value of 20 and 20 since they provide good distribution of solutions for the algorithm operations. Since the problem is separated into two parts (see Section V), the number of individuals in the population $(Pop_{num})$ and generations $(Gen_{num})$ are different in each case and therefore they are given in sections V-A and V-B.

In order to achieve the required constraints different ways exist in genetic algorithms [17]. The penalty function approach [18] is used to achieve the required constraints within limits, while the dynamically updated penalty functions are efficiently used to avoid infeasible solutions [19].

## V. FAULT TOLERANT CONTROL FOR AIR-GAP SENSOR FAILURE

The problem considered in this paper is to recover the performance of the MAGLEV suspension in case of a faulty air gap measurement (being a critical measurement). The technique used is depicted in Fig. 5. The non-linear model has three outputs. The air gap (G), the flux (B) and the current (I). Note that the scheme is implemented on the nonlinear model,



Authorized licensed use limited to: LOUGHBOROUGH UNIVERSITY. Downloaded on July 16, 2009 at 08:31 from IEEE Xplore. Restrictions apply.

while the appropriate linear signals are derived and fed to the linear system points for correct operation [20].
In order to detect a fault at the air gap measurement three air gap signals are compared. The measured air gap $(z_t - z)_{mea}$, the estimated air gap $(z_t - z)_{est}$ and the calculated air gap $(z_t - z)_{calc}$. The latest is calculated from (see [10])

$$(z_t - z)_{calc} = K_b \frac{I}{B} - G_o \tag{11}$$

Fault Detection and Isolation mechanisms compare the three signals and the residuals indicate if the actual gap measurement ($(z_t - z)_{mea}$) is healthy or not. In a healthy situation the air gap signal is given by

$$(z_t - z) = \left[(z_t - z)_{mea} + (z_t - z)_{est} + (z_t - z)_{calc}\right]/3 \tag{12}$$

When the air gap measurement becomes faulty, the faulty air gap measurement is isolated and the air gap signal $(z_t - z)$ is given by

$$(z_t - z) = \left[(z_t - z)_{calc} + (z_t - z)_{est}\right]/2 \tag{13}$$

The problem is separated in two parts. In the first part, the classical control strategy is optimised via NSGAII and the second part is automatic tuning of the Kalman filter to estimate the air gap $(z_t - z)_{est}$ signal using the current $(i)$ and the flux $(b)$ measurements.

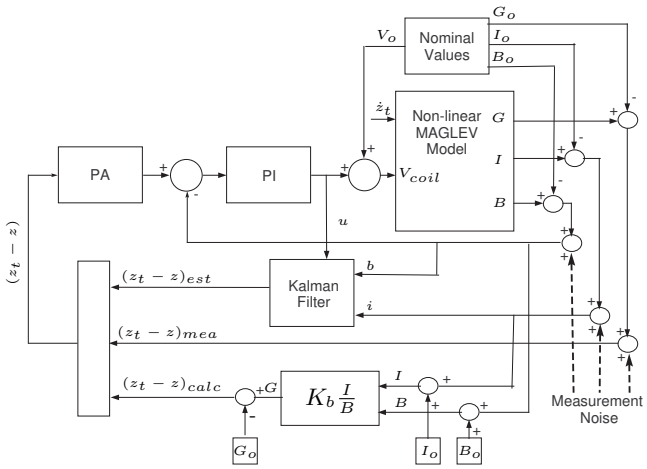


Fig. 5. Fault tolerant control scheme for air gap sensor failure for the MAGLEV suspension (nonlinear).

### A. Classical controller with inner loop design

In order to achieve fault-free performance a similar scheme to the one illustrated in Fig. (5) is used. Particularly, only the measured air gap $((z_t - z)_{mea})$ and flux $(b)$ are fed to the controllers. For the best possible rejection of the disturbance $\dot{z}_t$ and minimisation of the objectives while maintaining the suspension within the safe limits mentioned in section III-C, the parameters of the controllers are optimised via NSGAII. The control strategy uses a Proportional-Integral controller (PI) for the inner loop with a bandwidth in the range $50Hz - 100Hz$ while the outer loop is aimed at less than $10Hz$ using the phase advance controller (PA). The PA controller in equation (14), with $k$ the advance ratio and $\tau$ the time constant, is used to provide adequate phase margin in the range of $35^o - 45^o$.The controller's transfer functions are given as

$$PI = G_i \frac{t_i s + 1}{t_i s} \qquad PA = G_o \frac{k\tau s + 1}{\tau s + 1} \tag{14}$$

The controller parameters are tuned simultaneously via the evolutionary algorithm NSGAII and an optimum Pareto front of controllers is recovered. From those controllers that satisfy the predefined constraints, the desired controller that achieves the required performance can be selected.
The NSGAII parameters used are mentioned in section IV and the chromosome population is set to $Pop_{num} = 70$ for a maximum of 300 generations ($Gen_{num} = 300$).

### B. Kalman estimator tuning

The air gap measurement is included as a state in the linearised model of the MAGLEV system (see equation 3) and therefore a Kalman estimator can be used estimate it. Automatic tuning is performed via NSGAII as explained in section IV.
Consider the following state space expression which is the linearised MAGLEV model

$$\begin{aligned} \dot{x} &= A_g x + B_u u + B_w \omega_d \\ y &= C_m x + \omega_n \end{aligned} \tag{15}$$

where, $\omega_d$ and $\omega_n$ are the process and measurement noises respectively. These are assumed to be uncorrelated zero-mean Gaussian stochastic processes with constant power spectral densities $W$ and $V$ respectively.
The Kalman filter has the structure of an ordinary state-estimator with a state equation as

$$\dot{\hat{x}} = A\hat{x} + Bu + K_f(y - C\hat{x}) \tag{16}$$

where in this case, $A = A_g$, $B = B_u$ and $C = C_m$.
The optimal choice of $K_f$ via $W$ and $V$ minimises $E\{[x - \hat{x}]^T[x - \hat{x}]\}$ [21]. The optimum choice of $W$ and $V$ eventually controls the precision of the state estimation and therefore the evolutionary algorithm is used to tune the Kalman filter in order to give the same estimated air-gap as the actual measurement for both deterministic and stochastic responses. The noise covariance matrix $V$ is selected to be, diagonal $2 \times 2$ matrix with values of the noise covariance for the current and flux measurements, i.e $V = diag(V_i, V_b)$ ($V_i$ and $V_b$ are taken as the square of 1% of the maximum value for the deterministic response).
The $W$ matrix is given as $W = diag(W_i, W_{\dot{z}}, W_{(z_t - z)})$ where W is a $3 \times 3$ process noise matrix directly affect each states ($B_w = 3 \times 3$).
In order to estimate the air gap signal two objectives are selected to be minimised by the NSGAII. i.e to tune the Kalman filter presented in equation (17) and the Integral absolute error between the actual air-gap and the estimated for both deterministic ($\phi_{det}$) and stochastic ($\phi_{stoch}$) responses. Although the Kalman filter is stable by default it was important



Authorized licensed use limited to: LOUGHBOROUGH UNIVERSITY. Downloaded on July 16, 2009 at 08:31 from IEEE Xplore. Restrictions apply.

to take the appropriate time domain signal comparison for performance test.

$$\begin{aligned}\phi_{det} &= \int |(z_t - z)_{mea} - (z_t - z)_{est}|dt \\ \phi_{stoch} &= \int |(z_t - z)_{mea} - (z_t - z)_{est}|dt\end{aligned} \tag{17}$$

In this case, it is important to have a good precision for the estimated air-gap and therefore two constraints are assigned so that the precision is better than 5% ($\leq 5\%$) (18).

$$\begin{aligned}\omega_{det} &= \int |(z_t - z)_{mea} - (z_t - z)_{est}|dt \leq 0.05 \\ \omega_{stoch} &= \int |(z_t - z)_{mea} - (z_t - z)_{est}|dt \leq 0.05\end{aligned} \tag{18}$$

The parameters for the NSGAII are the same as mentioned in section IV but in this case, in order to reduce the computation effort, the chromosome population is set to $Pop_{num} = 50$ and the maximum generations to $Gen_{num} = 100$.

## VI. Simulations

The classical control approach used was successfully tuned and the desired performance of the MAGLEV suspension has been achieved. In Fig.6 the optimum Pareto front of controllers is illustrated. Although there are three assigned objectives, the trade-off between the $i_{rms}$ and $\ddot{z}$ is depicted that is of interest. A 3-D figure is avoided because the trade-off is not clear due to the nature of such plot. However, the 2-D plot is sufficient to show the Pareto-optimality of the important objectives ($i_{rms}, \ddot{z}$) while the maximum level of the noise is restricted to around $25V_{rms}$. This seams high value but as explained in section III-C the noise is filtered from the dynamics (see Fig. 7).
The ride quality of the suspension is less than $0.5m/s^2$ while the current from the stochastic behaviour is limited to around 1A. From the optimum Pareto front of controllers depicted in Fig. 6 all controllers shown are tuned to satisfy all constraints listed in Table I and therefore any one of them can be selected based on the user's requirements. The controllers that results in the best ride quality (smallest $\ddot{z}$) which is given in (19) is selected.

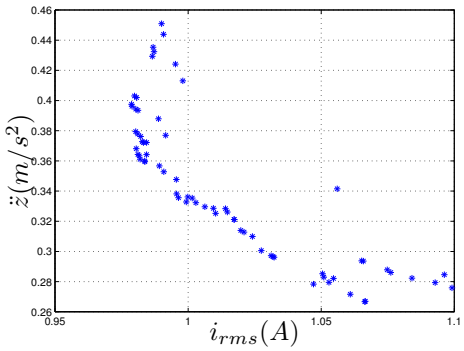


Fig. 6. Pareto front of controllers using NSGAII.

$$PA = 3.98\frac{0.1323s+1}{0.0244s+1} \quad PI = 1.1642e3\frac{0.0052s+1}{0.0052s} \tag{19}$$

The resulting ride quality is $0.26m/s^2$ and the air gap deviation on the track gradient is shown in Fig. 7(a). As it is shown, all the constraints for the deterministic response are satisfied including maximum air gap deviation and settling time. It is clear that the noise on the control effort (Fig.7(b)) does not affect the performance of the suspension and the maximum peak value constraint is satisfied.

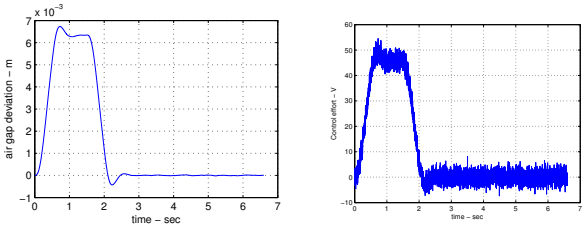


(a) deterministic response of air gap ($z_t - z$). (b) deterministic response of the input voltage ($u$).

Fig. 7. Deterministic response of air gap and control effort.

Using the proposed optimisation method, the controllers are successfully tuned and the next stage is to show that the Kalman filter is also able to estimate the air gap signal using only the current ($i$) and the flux ($b$) measurement. The Kalman filter has been tuned as explained in section V-B to estimate the air gap for both deterministic and stochastic responses. Figure 8 shows the error between the measured and the estimated ($e_{(z_t-z)_{mea,est}}$) and the measured and calculated ($e_{(z_t-z)_{mea,calc}}$) air gap signals for the deterministic response. The same results are obtained with the stochastic track inputs but are not illustrated here. In both cases the errors are small and therefore they can be used for the fault detection. The next step is to inject a fault in the actual air gap measurement and observe the results. In this case the fault scenario is that the actual air gap measurement sensor suddenly is damaged at $t = 1s$ and the output varies around zero in the form of a undesired coloured noise disturbance. The three air gap signals with the measured air gap signal which fails at $t = 1s$ are depicted in Fig.9(a). Figure 9(b) shows the difference between the actual air gap with no fault and with faulty air gap measurement. As can been seen, the performance of the suspension is successfully recovered with the actual air gap been fully recovered. The same results appears with stochastic inputs.

## VII. Conclusion

In this paper, a method has been proposed to recover the performance of a MAGLEV suspension in case of a faulty air gap sensor. In this case, no hardware redundancy is required for the air gap measurement thus reducing cost of the overall control system. The air gap measurement is rather critical for the maglev suspension system controllers, can be expensive and also located in harsh environment i.e increasing fault probability. A simplified, albeit robust control structure was proposed while the estimator successfully estimates the required signals for the fault tolerant structure. Simulation results



Authorized licensed use limited to: LOUGHBOROUGH UNIVERSITY. Downloaded on July 16, 2009 at 08:31 from IEEE Xplore. Restrictions apply.

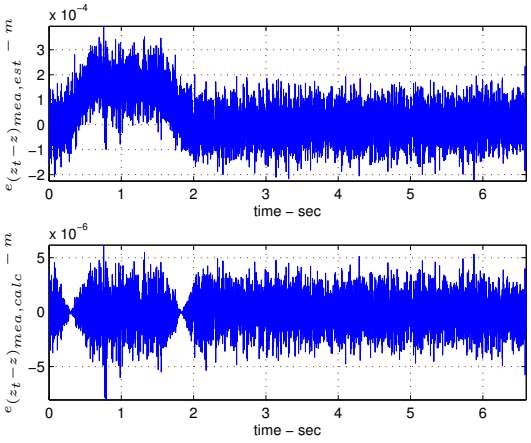


Fig. 8. Error between the measured and estimated ($e_{(z_t-z)_{mea,est}}$) and measured and calculated ($e_{(z_t-z)_{mea,calc}}$) air gap signals for the deterministic response.

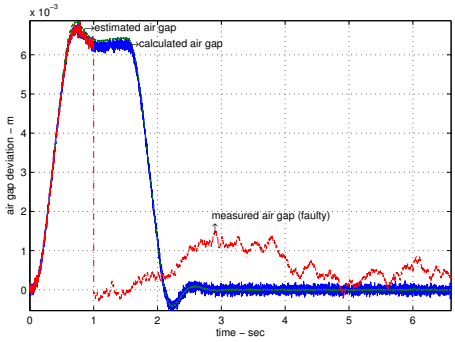


(a) The two air gap signals, and the faulty air gap measurement.

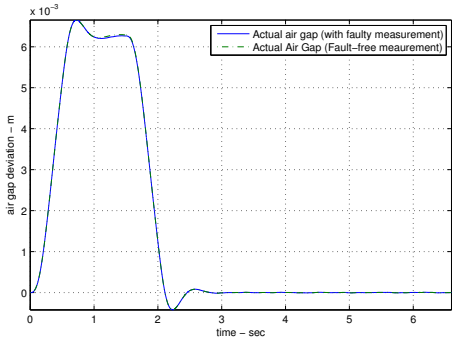


(b) Actual air gap signal for fault and fault-free air gap measurement.

Fig. 9. Air gap signals.

on the non-linear equivalent model illustrated the efficacy of the scheme.

## ACKNOWLEDGMENT

This work was supported in part under the EPSRC project Grant Ref. EP/D063965/1 and the Systems Engineering Innovation Centre at Loughborough University.

## REFERENCES

[1] H.-W. Lee, K.-C. Kim, and J. Lee, "Review of maglev train technologies," *IEEE Transactions on Magnetics*, vol. 42, no. 7, pp. 1917–1925, 2006.

[2] M. Blanke, C. W. Frei, F. Kraus, R. J. Patton, and M. Staroswiecki, "What is fault-tolerant control?" *Fault Detection, Supervision and Safety for Technical Processes 2000 (SAFEPROCESS 2000), Proceedings volume from the 4th IFAC Symposium*, pp. 40–51, 2001.

[3] C. Huixing, L. Zhiqiang, and C. Wensen, "Fault tolerant control research for high-speed maglev system with sensor failure," in *Sixth World Congress on Intelligent Control and Automation*, vol. 1, June 21-23 2006, pp. 2281–2285.

[4] H. K. Sung, S. H. Lee, and Z. Bien, "Design and implementation of a fault tolerant controller for ems systems," *Mechatronics,*, vol. 15, no. 10, pp. 1253–1272, 2005.

[5] Z. Zhang, Z. Long, L. She, and W. Chang, "Fault-tolerant control for maglev suspension system based on simultaneous stabilization," in *IEEE International Conference on Automation and Logistics, ICAL 2007*, 18-21 Aug 2007, pp. 299–303.

[6] H.-J. Kim, C.-K. Kim, and S. Kwon, "Design of a fault-tolerant levitation controller for magnetic levitation vehicle," in *International Conference on Electrical Machines and Systems, ICEMS 2007*, 8-11 Oct 2007, pp. 1977–1980.

[7] K. Michail, A. Zolotas, and R. M. Goodall, "Optimised sensor configurations for a maglev suspension," *Proceedings of the* $17^{th}$ *World Congress The internetional Federation of Automatic Control*, pp. 8305–8310, July 6-11, 2008.

[8] K. Michail, A. C. Zolotas, R. M. Goodall, and J. T. Pearson, "Maglev suspensions - a sensor optimisation framework," in *16th Mediterranean Conference on Control and Automation*, June 25-27 2008, pp. 1514–1519.

[9] K. Michail, A. Zolotas, R. M. Goodall, and J. T. Pearson, "Sensor optimisation via $h_\infty$ applied to a maglev suspension system." in *WASET ICCAS 2008: International Conference on Control and Automation Systems*, July 25-27 2008.

[10] R. M. Goodall, "Electromagnetic suspension control without airgap measurement," *Transactions of the Institute of Measurement and Control*, vol. 11, no. 2, pp. 92–98, 1989.

[11] P. J. Fleming and R. C. Purshouse, "Evolutionary algorithms in control systems engineering: A survey," *Control Engineering Practice*, vol. 10, no. 11, pp. 1223–1241, 2002.

[12] K. Deb, A. Pratap, S. Agarwal, and T. Meyarivan, "A fast and elitist multiobjective genetic algorithm: Nsga-ii," *IEEE Transactions on Evolutionary Computation*, vol. 6, no. 2, pp. 182–197, 2002.

[13] R. M. Goodall, "Generalised design models for ems maglev," in *Proceedings of MAGLEV 2008 - The* $20^{th}$ *International Conference on Magnetically Levitated Systems and Linear Drives*, 15-18 Dec 2008.

[14] R. M. Goodall, "Dynamics and control requirements for ems maglev suspensions," in *Proceedings on international conference on Maglev*, 2004, pp. 926–934.

[15] R. M. Goodall, "Dynamic characteristics in the design of maglev suspensions," *Proceedings of the Institution of Mechanical Engineers, Part F: Journal of Rail and Rapid Transit*, vol. 208, no. 1, pp. 33–41, 1994.

[16] R. M. Goodall, "On the robustness of flux feedback control for electromagnetic maglev controllers," in *Proceedings of 16th International Conference on MAGLEV Systems and Linear Drives*, 2000, pp. 197–202.

[17] C. A. C. Coello, "Theoretical and numerical constraint-handling techniques used with evolutionary algorithms: A survey of the state of the art," *Computer Methods in Applied Mechanics and Engineering*, vol. 191, no. 11-12, pp. 1245–1287, 2002.

[18] K. Deb, *Multi-objective Optimization using Evolutionary Algorithms*. John Wiley and sons Ltd, 2001.

[19] J. A. Joines and C. R. Houck, "On the use of non-stationary penalty functions to solve nonlinear constrained optimization problems with ga's," in *Proceedings of the First IEEE Conference on Evolutionary Computation*, vol. 2, 1994, pp. 579–584.

[20] B. Friedland, *Advanced Control System Design*. Prentice-Hall Inc., 1996.

[21] S. Skogestad and I. Postlethwaite, *Multivariable Feedback Control Analysis and Design*. John Wiley and Sons,Ltd, 2005.



Authorized licensed use limited to: LOUGHBOROUGH UNIVERSITY. Downloaded on July 16, 2009 at 08:31 from IEEE Xplore. Restrictions apply.